REDUCE, REUSE, RECYCLE: EVALUATING THE CONTRIBUTION OF *EUTREMA SALSUGINEUM* BYPASSES FOR GLYCOLYTIC SUBSTRATE LEVEL PHOSPHORYLATION IN RESPONSE TO LOW PHOSPHATE CONDITIONS

By

MADELINE MACLEAN

A Thesis

Submitted to the School of Interdisciplinary Science

In Partial Fulfilment of the Requirements

for the Degree

Bachelor of Science

McMaster University

BACHELOR OF SCIENCE (2024) McMaster University

School of Interdisciplinary Science Hamilton, Ontario

TITLE: Reduce, Reuse, Recycle: Evaluating the contribution of *Eutrema salsugineum* bypasses for glycolytic substrate level phosphorylation in response to low phosphate conditions

AUTHOR: Madeline MacLean

SUPERVISOR: Dr. Elizabeth Weretilnyk

NUMBER OF PAGES: 32

Abstract

Drought reduces the availability of dissolved nutrients for plant uptake. For the essential macronutrient phosphate (Pi), drought exacerbates its already low soil availability for plant uptake. Understanding the mechanisms allowing plants to thrive under semi-arid, low-Pi conditions enables us to develop climate change resilient crops less reliant on added Pi fertilizers. *Eutrema salsugineum* is an extremophile plant and the Yukon ecotype thrives on low-Pi soil. Yukon plants can bypass glycolytic glyceraldehyde 3-phosphate dehydrogenase (GAPDH) using NADH and Pi to phosphorylate ADP by employing a non-phosphorylating (NP) GAPDH. By avoiding phosphorylation, NP-GAPDH can preserve Pi for alternative use in a deficient plant. The Shandong ecotype is less tolerant of low Pi, so their capacity to use the bypass was also evaluated. GAPDH and NP-GAPDH activity was measured in leaf and root cell-free extracts of plants grown with (+Pi) or without Pi (-Pi). For both ecotypes, up to 10-fold higher activity rates were found in leaf extracts relative to root extracts. In -Pi plants, leaf GAPDH activity was approximately three-fold and two-fold greater relative to +Pi plants for Yukon and Shandong respectively. Leaf NP-GAPDH activity was slightly greater in +Pi relative to -Pi in Yukon plants, while rates were comparable for -Pi and +Pi Shandong plants. Furthermore, NP-GAPDH activity in Yukon and Shandong plants were similar, suggesting that the bypass does not play an essential role for tolerance to low-Pi conditions and raises a question about the true metabolic role of this enzyme in plants.

Acknowledgements

I would like to thank Dr. Elizabeth Weretilnyk for supervising me throughout this entire process. Your constant support pushed me to keep going even when I was struggling, and I learned a lot of valuable lessons in addition to all the science. I would not have made it through this project without your countless hours of meetings and revisions on my presentation and final paper. I am so grateful to Dr. Peter Summers for training me on every procedure I performed in the lab, for answering every question I had, for helping me troubleshoot calculations, and for spending so many hours in the lab to make sure help was available if it was needed. I am thankful for Laura Li for answering every uncertain question I had and Haoran Jia for providing *Eutrema* transcriptome data, and to both for making the lab feel like a place where I belonged and could succeed. Furthermore, I could not have completed this project without previous student Jess Latimer's leftover plant materials, Vera Velasco's previous data and study direction, and Heather Summers for her help with R. Finally, I am so grateful to my fellow undergraduates Sofia Di Francesco and Avery Murphy for their moral support and camaraderie, as I would not have made it through without my friends pushing through alongside me.

Table of Contents

List of Figures

List of Tables

Glossary

3-PGA	(3-phosphoglycerate)
µL	(microlitre(s))
µmol	(micromole(s))
ADP	(adenosine diphosphate)
ATP	(adenosine triphosphate)
C	(Celsius)
Cat. No.	(catalogue number)
cGAPDH	(cytosolic phosphorylating glyceraldehyde-3-phosphate dehydrogenase)
dH_2O	(deionized water)
DTE	(dithioerythritol)
DTT	(dithiothreitol)
EDTA	(ethylenediaminetetraacetic acid)
FW	(fresh weight)
g	(grams)
GAPDH	(glyceraldehyde-3-phosphate dehydrogenase)
gFW	(grams of fresh weight)
HD	(HEPES and DTT)
HED	(HEPES, EDTA, and DTT)
HEPES	(4-(2-hydroxyethyl)-1-piperazineethanesulfonic acid)
mg	(milligram(s))
mgprot	(milligrams of protein)
min	(minutes)
mL	(millilitre(s))
mM	(millimolar)
mm	(millimetre(s))
n	(sample size)

NAD(H)	(nicotinamide adenine dinucleotide)
NADP(H)	nicotinamide adenine dinucleotide phosphate
nm	(nanometre(s))
nmol	(nanomole(s))
No.	(number)
NP-GAPDH	(non-phosphorylating glyceraldehyde-3-phosphate dehydrogenase)
pH	(potential of hydrogen)
Pi	(inorganic phosphate)
PPK	(polyphosphate kinase)
PVP 40000	(polyvinylpyrrolidone average molecular weight 40000)
Ref.	(reference number)
rpm	(revolutions per minute)
T2299	(*Eutrema salsugineum* Yukon ecotype seed line)
T2350	(*Eutrema salsugineum* Shandong ecotype seed line)

Introduction

As the climate changes, so too do agricultural environments. New challenges have arisen for crop production, such as decreased precipitation, soil degradation and nutrient deficiency, higher temperatures, and an increase in soil salinity. Drought is responsible for approximately 50% of annual abiotic crop yield loss (MacLeod et al., 2015). Furthermore, soil degradation and salinity often work in tandem, with the increased presence of salts inhibiting uptake and translocation of the already diminished available mineral nutrients (Lv et al., 2021). One especially important nutrient, inorganic phosphate (Pi), is vital for plant growth and development, but is often limiting in soil (Velasco et al., 2016).

Pi is available in relatively high concentrations in soil, but the majority of it exists in mineral form having bonded with cations such as aluminum and iron and thus cannot be taken up reliably by the plants (Vance, Uhde-Stone and Allan, 2003). This has led to Pi acting as a limiting nutrient for crop health in up to 40% of viable agricultural land (Vance, Uhde-Stone and Allan, 2003). While the usage of Pi fertilizer has attempted to mitigate this issue, the excessive reliance on it is depleting the non-renewable rock-based Pi resources and polluting the environment (Plaxton and Tran, 2011; Velasco et al., 2016; Wang et al., 2017). It is clear that new strategies must be developed in order to combat these new challenges; one such current strategy is studying model organisms already adapted to abiotic stress to identify how they survive their extreme conditions and if these traits can be transferred to other organisms (Amtmann, 2009).

Eutrema salsugineum and its Ecotypes

Eutrema salsugineum (formerly *Thellungiella salsuginea*, commonly salt cress), a close relative of *Arabidopsis thaliana* and member of the Brassicaceae family, is one such model organism (Amtmann, 2009; Ariga et al., 2015; Yeo et al., 2015). *Eutrema* is an extremophile that is tolerant of drought (Guevara et al., 2012; MacLeod et al., 2015), salinity (Guevara et al., 2012; Ariga et al., 2015; Kazachkova et al., 2016; Kazachkova et al., 2018), extreme cold (Griffith et al., 2007; Guevara et al., 2012; Ariga et al., 2015), limited nitrogen and Pi (Kazachkova et al., 2018), and pathogen stress (Yeo et al., 2015).

Eutrema has two main ecotypes that have been studied extensively, with one ecotype native to Yukon Territory, Canada and the other native to Shandong, China. The two ecotypes express similar capacities to tolerate abiotic and biotic stress; however, their native environments are so different that it is unlikely that these tolerances were developed the same way (Yeo et al., 2015). In the Yukon, the climate is semi-arid and sub-Arctic with a short growing season, resulting in drought, extreme temperatures, and severe temperature fluctuations (Amtmann, 2009; MacLeod et al., 2015). Additionally, Yukon soils are saturated with sodium chloride, calcium carbonate, and magnesium sulfate, low in Pi as a result of being suspended in mineral forms that the plant cannot take up, and the layer of permafrost near the top of the soil reduces the ability of soil microorganisms to perform mineralization (Velasco et al., 2019). The Shandong ecotype, however, grows on a high-salinity coast under a warm, temperate climate with monsoonal precipitation seasons (MacLeod et al., 2015; Khanal et al., 2017). Yin et al. (2018) attempted to identify the cause of the morphological and stress tolerance differences between the two ecotypes through transcriptome analysis. While they were able to find 31 genes

that differed between them, none were able to explain the physiological or morphological differences that the two ecotypes expressed (Yin et al., 2018).

Metabolic Adaptations

Glycolysis is an essential metabolic pathway for every type of organism, as it converts sugars into usable compounds and generates ATP for energy within the cell (Givan, 1999). In order to make this process function, organisms require a lot of Pi. Substrate level phosphorylation involves the enzymes glyceraldehyde phosphate dehydrogenase (GAPDH) using NAD and Pi to produce 1,3 bisphosphoglycerate followed by phosphoglycerate kinase that phosphorylates ADP to produce ATP (Givan, 1999). However, in order for organisms to adapt to and survive under conditions lacking sufficient Pi, they must have a way to use their limited Pi resources sparingly and efficiently.

Glycolysis rates in rat muscle can increase significantly in the presence of non-phosphorylating glyceraldehyde-3-phosphate dehydrogenase (GAPN) (Arutyunov and Muronetz, 2003). When rat muscle is at a deficit of ADP and cytosolic Pi, GAPN is able to catalyze the oxidation of glyceraldehyde-3-phosphate to 3-phosphoglycerate and, concurrently, reduce NAD(P) (Arutyunov and Muronetz, 2003). GAPN activity is also found in bacterial glycolytic pathways; while all bacterial domains were found to have GAPDH, most archaea bacteria also possess GAPN (Ito et al., 2012).

Archae bacteria use GAPN in the same way as the rat muscle, namely for oxidizing glyceraldehyde-3-phosphate to 3-phosphoglycerate and bypassing the need to generate ATP (Ito et al., 2012; Zhang et al., 2017). Additionally, a similar pathway was found in the *Euryarchaeota* bacteria *Thermococcus kodakarensis* and *Pyococcus furiosus* (Matsubara et al., 2011). In the

latter bacterial examples, none encoded GAPDH or GAPN, but possessed another alternate route altogether (Matsubara et al., 2011). In plants, very little information about GAPN or similar mechanisms has been found, but recent research by Vera Velasco et al. (2016; 2019) on low Pi tolerance in *Eutrema* may hold some answers.

Glycolytic Bypasses In Eutrema

Eutrema is adapted to soils with moderate to low Pi availability and has adapted multiple processes to overcome this deficit, but they are not necessarily the expected mechanisms. Common mechanisms plants use to cope with limited Pi include root elongation, lateral root proliferation, and increased root hair density, as these are all mechanical ways for a plant to increase its Pi uptake (Velasco et al., 2016). However, when Yukon *Eutrema* was exposed to varying levels of Pi concentrations on media plates, no significant change in lateral root density or shoot biomass allocation was observed (Velasco et al., 2016). The authors theorized that since *Eutrema* is chronically exposed to low Pi levels, it had developed alternate forms of managing Pi usage (Velasco et al., 2016).

Further studies on the Yukon ecotype were able to confirm that some root-associated traits and metabolic processes were likely responsible for the plant's ability to retrieve, use, and recycle Pi efficiently (Velasco et al., 2019). Root modifications such as root hairs or cluster roots can improve Pi scavenging capabilities when there is limited Pi available, while metabolic flexibility is a less permanent adaptation that allows for Pi reuse and preservation through the avoidance of ATP and generation of free Pi (Velasco et al., 2019).

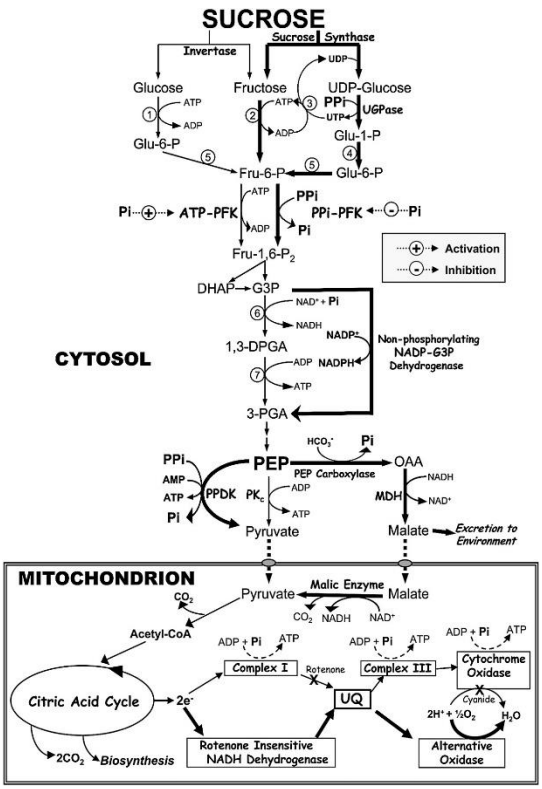

Figure 1: Diagram showing the main glycolysis pathway (straight down) and the multiple bypasses throughout (outside arrows) that allow the organism to preserve Pi (Plaxton and Tran, 2011).

Velasco et al. (2019) found that the Yukon ecotype of *Eutrema* uses three main glycolytic bypasses to preserve Pi within the plant: UDP-glucose pyrophosphorylase and pyrophosphate-dependent phosphofructokinase bypass hexokinase and ATP-dependent phosphofructokinase reactions; non-phosphorylating glyceraldehyde-3-phosphate dehydrogenase (NP-GAPDH), similar to GAPN mentioned previously, bypasses cytosolic GAPDH; and phosphoenolpyruvate carboxylase (PEPC), malate dehydrogenase, and malic enzyme work together to release Pi from PEP and maintain PEP to pyruvate flux when ADP is limiting to bypass cytosolic pyruvate kinase. Each of these pathways preserves Pi on its own, but by combining all three together, *Eutrema* is able to make the most of its limited resources.

Conclusion

Velasco et al.'s work on identifying metabolic adaptations to low Pi stress in *Eutrema* is a strong start to understanding a potential pathway for enhancing low Pi stress tolerance in crops. However, there is still much to be discovered in this vein. Currently, the capacity for operating metabolic bypass pathways in Shandong plants is unknown , and each step in the glycolytic pathway should be studied to determine the role that each bypass plays in the overall picture of stress tolerance. I will be using Velasco et al (2019) as a jumping-off point for my thesis.

Objective and Hypothesis

This thesis project aimed to investigate one of *Eutrema*'s key adaptations to surviving in low-Pi environments: the usage of NP-GAPDH to bypass GAPDH and ATP and preserve Pi levels within the plant. As there is very little research in this area, the guiding research questions were aimed towards learning new information rather than verifying previous claims. NP-GAPDH activity was examined to determine whether it is significantly greater than cGAPDH activity in Yukon and Shandong *Eutrema* grown under low vs Pi-fertilized conditions. If Shandong *Eutrema* were able to use NP-GAPDH, their enzyme activity levels would be compared relative to Yukon plants. As genes encoding NP-GAPDH have not been reported, the genetic database Phytozome was used to determine the number of genes encoding the NP-GAPDH pathway and transcriptome data available in the Weretilnyk lab was analyzed to determine the expression levels of these genes.

It was hypothesized that both Yukon and Shandong plants would have the capacity to use the NP-GAPDH pathway, but that Yukon plants would have a greater capacity for this it than Shandong plants. No significant difference between the NP-GAPDH produced between -Pi and +Pi for either ecotype was anticipated, but it was believed that Shandong -Pi plants may show a lower capacity to thrive on low Pi.

Methods and Materials

Plant Material

Yukon and Shandong *Eutrema* material that was generated by a previous member of the Weretilnyk lab was used for all experiments. The Yukon plants were grown from seed line T2299 and Shandong plants were grown from seed line T2350, the numerical codes corresponding to the seed lines in the lab catalogue.

Preparing Grind Buffer

The buffer for tissue grinding as described by Hurley et al. (2010) was prepared in a 50 mL beaker containing 25 mL of dH_2O and a magnetic stir bar. 596 mg of HEPES (100 mM), 100 µL of 250 mM of Na_2-EDTA (1 mM), 22 mg of ascorbic acid (5 mM), 15.4 mg of boric acid (10 mM), 9.5 mg of sodium metabisulphite (20 mM), and 19.3 mg of DTT (5 mM) were added and stirred. Once mixed, the buffer was brought to pH 7.8 through dropwise additions of 5N and 1N KOH. The Thermo Scientific Orion Star Series pH meter (Serial No. E03467) and the AquaPro Triode probe (Orion 9107APMD) was used to monitor pH. 1 g of PVP 40000 was added and stirred until completely dissolved.

Grinding Plant Tissue

A mortar and pestle were placed on aluminum foil on ice. Shoot and root sample tissue from Jess Latimer (2022-2023) was taken out of the -80°C freezer and placed in liquid nitrogen until ready to be ground. Liquid nitrogen was poured into the mortar and once only a thin layer

remained, the aluminum foil package containing the desired tissue sample was quickly unwrapped and transferred to the mortar. As described by Hurley et al. (2010), The tissue was ground into a fine powder as grind buffer was added to the frozen tissue until a buffer to tissue fresh weight ratio of 1:1 was reached for shoots and a ratio of 1.5:1 was reached for roots. As the powder turned to a slurry, grind buffer was added and used to rinse the mortar until a buffer to tissue fresh weight ratio of 2:1 was reached for shoots and a ratio of 3:1 was reached for roots. The final slurry was poured into labelled 1.5 mL microfuge tubes on ice and spun at 12000 rpm for three minutes at 4°C. This supernatant was transferred to fresh labelled 1.5 mL microfuge tubes on ice.

Preparing Sephadex G25 Desalting Columns

For cGAPDH assays, Sephadex G25 beads were suspended and stored in the 4°C fridge one day prior to grinding in HED buffer (2.383 g of HEPES, 1 mL of 100 mM Na_2-EDTA, and 77.1 mg of DTT in 100 mL of dH_2O and brought to pH 7.8 with KOH). This was performed in accordance with the protocol described in Summers and Weretilnyk (1993). For NP-GAPDH assays, Sephadex G25 beads were suspended and stored in the 4°C fridge one day prior to grinding in HD buffer (2.383 g of HEPES and 77.1 mg of DTT in 100 mL of dH_2O and brought to pH 7.8 with KOH). 1.7 g of Sephadex beads in 10 mL of buffer was enough to generate six columns.

Columns were made in 1.5 mL microfuge tubes. Lids were removed and tubes were placed inside 13 mm x100 mm test tubes. Swollen Sephadex G25 was added to a volume of 1.1 mL using a Pasteur pipette. A 25G x 5/8 (0.5 mm x 16 mm) BD PrecisionGlide™ needle (Ref.

305122) was used to poke a hole in the bottom of each microfuge tube to allow excess buffer to drain. Tubes were centrifuged for 12 seconds on max speed in the clinical centrifuge to draw excess buffer into the test tube. Successfully spun columns were transferred to clean 13 mm x 100 mm test tubes.

Desalting Tissue Extract

In accordance with Summers and Weretilnyk (1993), 180 µL of supernatant from the ground plant material was pipetted onto prepared Sephadex columns and spun for 12 seconds on max speed in the clinical centrifuge. The resulting desalted extract that had flowed through the column was transferred to a fresh and labelled 1.5 mL microfuge tube using a Pasteur pipette, flash frozen in liquid nitrogen, and stored at -80°C. Unused supernatant was also flash frozen in liquid nitrogen and stored at -80°C.

cGAPDH Assay

The cGAPDH assay was performed in accordance with the protocol outlined in Plaxton (1990). The assay buffer containing 40 µL of 500 mM HEPES-KOH pH 8 (100 mM), 2 µL of 1 M $MgCl_2$ (10 mM), 2 µL of 100 mM Na_2-EDTA (1 mM), 4 µL of 100 mM DTE (2 mM), 8 µL of 8 mM NADH (0.2 mM), 10 µL of 100 mM ATP (5 mM), 0.4 µL of units/mL PPK (2 µL per mL), and 103.6 µL of dH_2O was prepared as a soup at 10x volume to make enough solution for nine assays. Desalted plant material was diluted with 50 mM HEPES-KOH pH 8, with shoot material being diluted by a factor of 8 and root material being diluted by a factor of 5. 20 µL of dH_2O was added as a control to wells one to three of a flat-bottom 96-well MicroTest Plate (Cat. No.

82.1581, Sarstedt AG & Co., Nümbrecht, Germany). 170 µL of assay soup was added to each well, followed by 10 µL of diluted plant material. 20 µL of 2 mM 3-phosphoglyceric acid (3-PGA) was added to wells four to nine to start the reaction. The total volume in each well was 200 µL and wells were stirred gently with a pipette tip before reading to ensure proper mixing. The oxidation of NADH to NAD^+ was measured using the Multiskan Spectrum 1500 (Thermo Labsystems, Helsinki, Finland) plate reader, which measured absorbance at 340 nm every ten seconds for four minutes (24 readings).

NP-GAPDH Assay

The NP-GAPDH assay was performed in accordance with the protocol described by Rius et al. (2006). The assay buffer containing 20 µL of 500 mM HEPES-KOH pH 8 (50 mM), 40 µL of 2 mM NADP (0.4 mM), and 0.6 µL of 1 unit/mL aldolase (1 unit per mL) was prepared as a soup at 10x volume to make enough solution for nine assays. The aldolase was made fresh for each reaction by mixing crystalized aldolase with HED buffer to a concentration of 1 unit/mL HED. Desalted plant material was diluted by a factor of 5 with 50 mM HEPES-KOH pH 8. 130 µL of dH_2O was added as a control to wells one to three of a flat-bottom 96-well MicroTest Plate and 110 µL of dH_2O was added to wells four to nine. 60 µL of assay soup was added to each well, followed by 10 µL of diluted plant material. 20 µL of 12 mM fructose-1,6-bisphosphate (F16P2) was added to wells four to nine to start the reaction. The total volume in each well was 200 µL and wells were stirred gently with a pipette tip before reading to ensure proper mixing. The reduction of NADP to NADPH was measured using the Multiskan Spectrum 1500 plate reader, which measured absorbance at 340 nm every 60 seconds for 60 minutes (60 readings).

Bradford's Assay

25 µL of desalted extract was saved from every ground sample of plant material in order to determine its protein content using the Bradford's assay. A standard curve of known protein content was created using bovine serum albumin (BSA) standards starting at 0.5 mg/mL and serial diluted to 0.25 mg/mL, 0.125 mg/mL, 0.0625 mg/mL, 0.03125 mg/mL, and 0.0156 mg/mL. 100 µL of each standard solution was transferred into two 13 mm x 100 mm test tubes for technical replicates. This protocol was followed from Bradford (1976). Two test tubes were made containing 100 µL of dH_2O to act as a control. 700 µL of dH_2O was added to each test tube, followed by 200 µL of undiluted Bradford's reagent (Cat. No. 500-0006, Bio-Rad). Test tubes were vortexed immediately after the addition of the Bradford's reagent and let to stand for five minutes. 200 µL of each solution were transferred to a well in a flat-bottom 96-well MicroTest Plate and absorbance was measured at 595 nm using the Multiskan Spectrum 1500 plate reader. The absorbance of the control trials was subtracted from the absorbance of the BSA standards to remove background noise and the resulting values were used to create the standard curve.

20 µL of the saved desalted extract was diluted in dH_2O, with shoot material being diluted by a factor of 31 (600 µL dH_2O) and root material being diluted by a factor of 11 (200 µL dH_2O). 100 µL of each diluted desalted solution was transferred into two 13 mm x 100 mm test tubes for technical replicates. 700 µL of dH_2O was added to each test tube, followed by 200 µL of undiluted Bradford's reagent (Cat. No. 500-0006, Bio-Rad). Test tubes were vortexed immediately after the addition of the Bradford's reagent and let to stand for five minutes. 200 µL of each solution were transferred to a well in a flat-bottom 96-well MicroTest Plate and absorbance was measured at 595 nm using the Multiskan Spectrum 1500 plate reader. To

determine protein content of each sample, the absorbance reading of the dH_2O controls was subtracted from the absorbance readings of each run sample and the resulting values were input into the equation of the slope of the standard curve.

Calculating cGAPDH Activity

The measurements of NADH oxidation were converted to Microsoft Excel files. For each well, the change in absorbance was plotted and the slope of the line used to quantify cGAPDH activity. As the reaction results in a decrease in NADH, the slope will be negative, with a greater slope indicating greater activity. The average values for the control trials were subtracted from the average values for the experimental trials to generate the rate of activity (OD/min) of the sample. A standard curve of NADH concentration was used to convert OD/min to enzyme activity in ΔNADH/min. This value was then adjusted for dilutions and normalized by fresh weight and protein content.

Calculating NP-GAPDH Activity

The measurements of NADP reduction were converted to Microsoft Excel files. For each well, the change in absorbance was plotted and the slope of the line used to quantify NP-GAPDH activity. As the reaction results in an increase in NADPH, the slope will be positive, with a greater slope indicating greater activity. The average values for the control trials were subtracted from the average values for the experimental trials to generate the rate of activity (OD/min) of the sample. As NADH and NADPH have a similar absorbance value, the same standard curve

was used to convert OD/min to enzyme activity in ΔNADP/min. This value was then adjusted for dilutions and normalized by fresh weight and protein content.

Genetic Analysis

Phytozome version 13, the plant genomics resource, was used to determine how many genes were involved in the glycolysis IV pathway in *Eutrema*. The *Arabidopsis thaliana* gene known to be involved in the non-phosphorylating pathway was input into the gene search and used to find the *Eutrema* homologue. From there, the glycolysis IV pathway graphic containing all genes involved was consulted to determine the total number of genes involved in both the cytosolic and non-phosphorylating pathways.

Transcriptome data of Yukon and Shandong plants from the Weretilnyk lab was used to determine the gene expression of the identified genes from Phytozome. The transcriptome data compared levels of expression in low Pi versus high Pi conditions and low Pi with high nitrogen versus high Pi with high nitrogen conditions for both Yukon and Shandong plants and identified which genes were up or down regulated for each condition.

Results

cGAPDH Assay

Each treatment (-/+ Pi) of each ecotype (Shandong/Yukon) had at least three biological replicates, with a total of 28 (14 shoots/14 roots) plant material samples being assayed. Six technical replicates were measured for each sample with the mean value being used in

calculations. The results of the cGAPDH assays were reported in terms of both gFW (Figure 2) and mgprot (Figure 3) and were separated by treatment type. Results for gFW were up to 25-fold greater than the results for mgprot, but also showed more variance between data points. Shoots consistently showed greater rates of activity than roots. Rates of activity between Shandong and Yukon samples were similar and showed similar trends. -Pi shoot material displayed up to 3-fold greater rates of activity than +Pi shoot material in terms of mgprot, whereas the difference was less pronounced in gFW. Root material displayed little variance between -Pi and +Pi treatments.

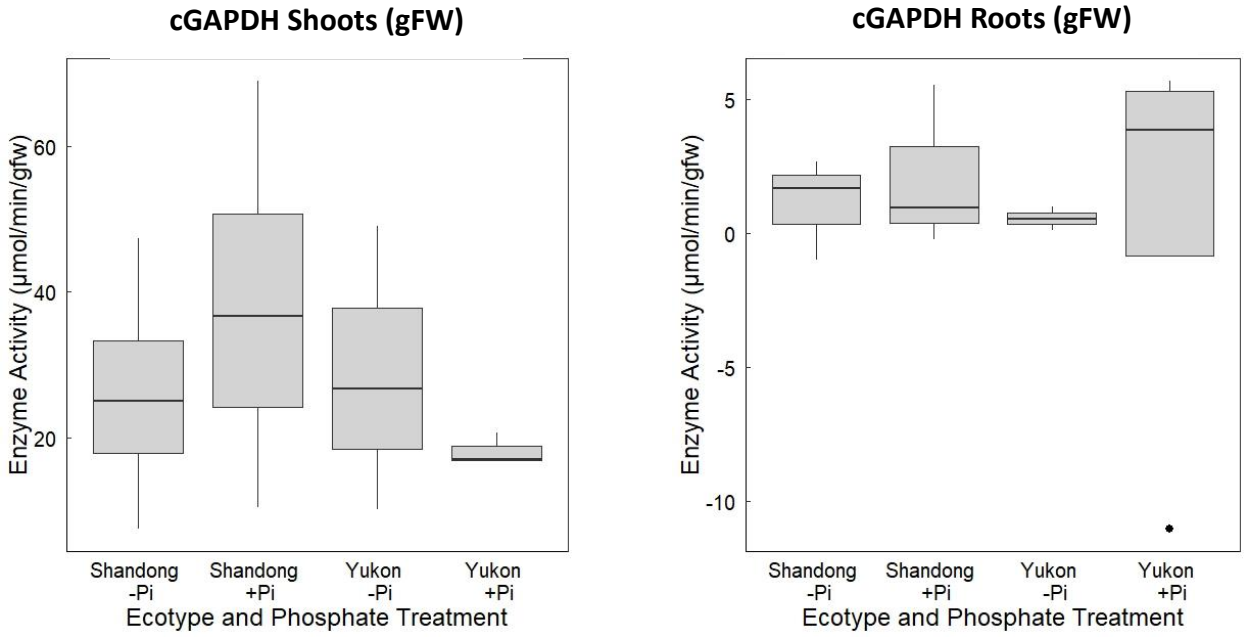

Figure 2: Boxplots denoting cGAPDH activity in µmol/min/gFW of desalted *Eutrema* shoots (left) and roots (right). n = 3 for all trials except Shandong +Pi shoots, Shandong -Pi roots, and Yukon +Pi roots which had n = 4. The black bar represents the mean of the sample group and the whiskers represent the 95% confidence interval. The singular point in the Yukon +Pi cGAPDH roots column is an outlier and was not included in the calculation for the 95% confidence interval. Enzyme activity was found to be similar in both shoots and roots across both ecotypes and treatments, as shown by the overlap by all boxes. The roots and Shandong shoots data shows that +Pi plants had a slightly greater capacity to use the pathway.

The gFW data shows a general trend of +Pi plants having an increased capacity to use the cytosolic pathway than -Pi plants, though this trend is not hugely significant as all the boxes are

overlapped which indicates that each treatment is functioning in the same range of activity. No significant difference in activity was seen between the two ecotypes either.

The mgprot data shows a more significant difference between Pi treatments in the shoots, with +Pi plants showing an up to two-fold greater rate of enzyme activity than -Pi plants. +Pi Shandong and Yukon plants were found to have similar rates of activity. Shandong -Pi shoots displayed a significantly greater rate of activity than Yukon -Pi shoots, as seen by the complete lack of overlap of 95% confidence interval ranges. In roots, rates of activity were much less variable and both ecotypes and Pi treatments showed no significant difference.

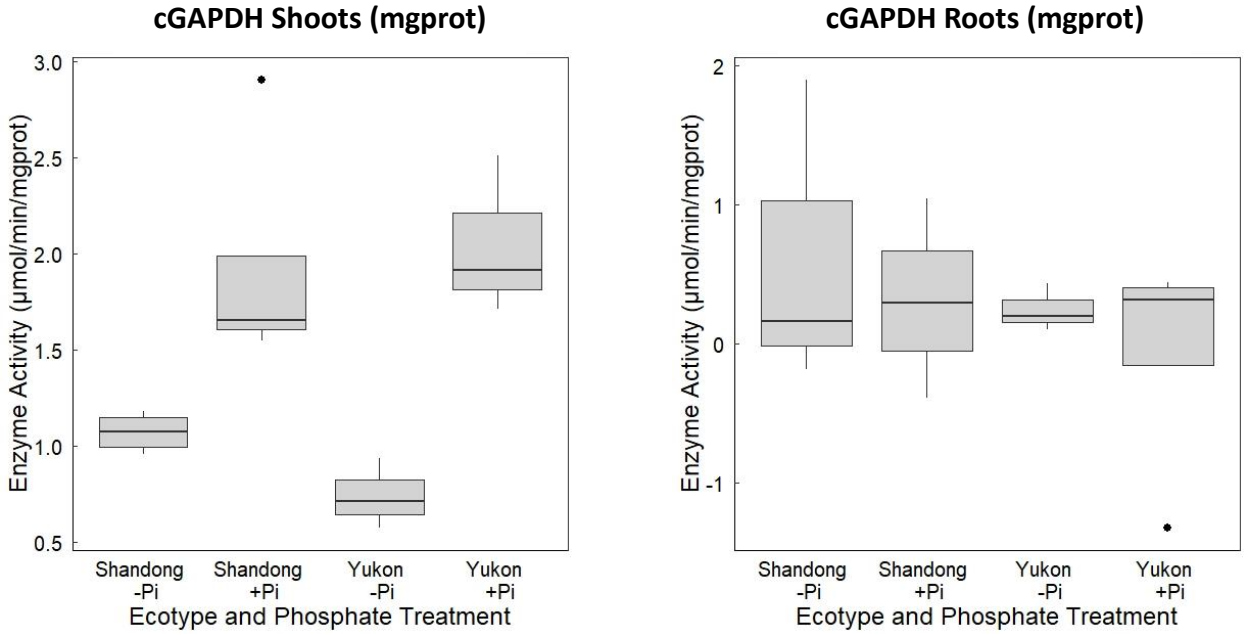

Figure 3: Boxplots denoting cGAPDH activity in µmol NADH/min/mgprot of desalted *Eutrema* shoots (left) and roots (right). n = 3 for all trials except Shandong +Pi shoots, Shandong -Pi roots, and Yukon +Pi roots which had n = 4. The black bar represents the mean of the sample group and the whiskers represent the 95% confidence interval. The singular point in the Shandong +Pi cGAPDH shoots and the Yukon +Pi cGAPDH roots column is an outlier and was not included in the calculation for the 95% confidence interval. Enzyme activity was similar between ecotypes for both shoots and roots. Roots data showed little variance in rates of activity, whereas shoots data showed a significant difference between -Pi and +Pi treatments.

NP-GAPDH Assay

The results of the NP-GAPDH assays were also reported in terms of both gFW (Figure 4) and mgprot (Figure 5) and were separated by treatment type. Rates of activity for gFW were up to 100-fold greater than rates for mgprot. Root samples showed very limited activity in both mgprot and gFW. Shandong material showed greater rates of activity than Yukon material in mgprot, but -Pi Yukon material in gFW displayed greater rates of activity than +Pi Yukon and both types of Shandong material. Shandong and Yukon material showed the same trend of activity between -Pi and +Pi when analyzed for gFW, with greater rates of activity being seen in -Pi than +Pi treatments. Shandong shoot material showed the same pattern for mgprot, whereas Yukon shoot material showed the opposite.

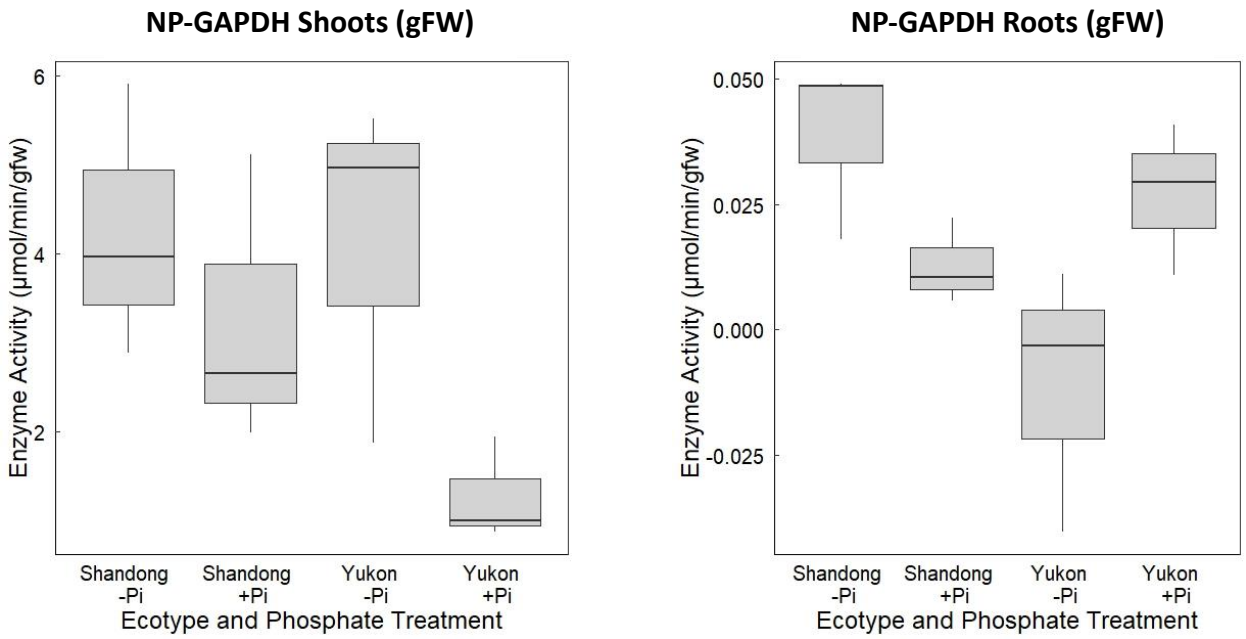

Figure 4: Boxplots denoting NP-GAPDH activity in µmol NADPH/min/gFW of desalted *Eutrema* shoots (left) and roots (right). n = 3 for all trials. The black bar represents the mean of the sample group and the whiskers represent the 95% confidence interval. Yukon -Pi roots data that is below 0.000 should be considered negligible. -Pi shoots data was significantly greater than +Pi shoots data, especially in Yukon plants. Roots showed significantly less activity than shoots.

Figure 4 reported greater activity in the NP-GAPDH pathway in -Pi shoots than in +Pi shoots for both Shandong and Yukon plants. In the Yukon shoots data, -Pi plants had up to 5-fold greater rates of activity than +Pi plants. Shandong shoots showed a similar trend, with -Pi plants displaying rates of activity up to 2-fold greater than +Pi plants. Shandong and Yukon -Pi shoots showed highly similar rates of activity, with the mean of Yukon shoots only slightly greater than the mean of Shandong shoots. gFW NP-GAPDH data for the roots was much less prominent in total activity, but Shandong plants showed a similar trend with -Pi plants generating more activity than +Pi plants. Yukon roots data is inconclusive, as little activity was recorded for -Pi plants. Yukon +Pi roots activity was up to 2-fold greater than Shandong +Pi activity, however.

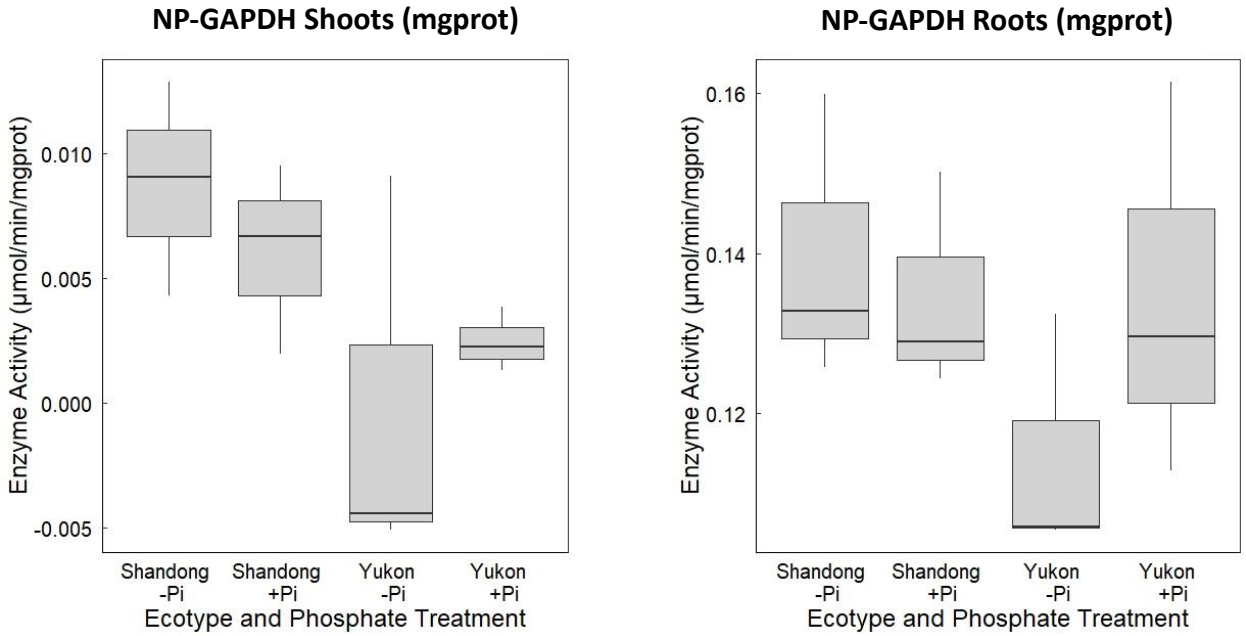

Figure 5: Boxplots denoting NP-GAPDH activity in µmol NADPH/min/mgprot of desalted *Eutrema* shoots (left) and roots (right). n = 3 for all trials. The black bar represents the mean of the sample group and the whiskers represent the 95% confidence interval. Yukon -Pi roots data that is below 0.000 should be considered negligible. Yukon -Pi shoots and roots showed limited rates of activity, while Yukon +Pi shoots and roots were much greater. Shandong plants showed greater rates of activity in -Pi treatments than in +Pi treatments.

The mgprot data reported above in Figure 5 shows a different pattern than the gFW data, with Yukon -Pi plants displaying a significantly decreased rate of activity for the NP-GAPDH pathway than +Pi plants in both shoots and roots. This lack of Yukon -Pi activity was anomolous and contradicted the expected outcome of the experiment. Shandong shoots and roots showed similar trends of activity in mgprot compared to in gFW, with -Pi plants having greater rates of activity than +Pi plants. Roots data again showed significantly less activity than shoots data and also shows less difference between rates of activity for both ecotypes and treatments.

Genetic Analysis

A total of 23 genes were found to contribute to the GAPDH pathway in *Eutrema* (Table 1). Nine of these genes were specific to the cytosolic pathway, whereas three of these genes were specific to the non-phosphorylating pathway. The other 11 genes are included in both pathways. These genes are reported in Tables 1-3 below. Transcriptome analysis of the 23 identified genes was inconclusive, as none of the found genes were represented in the transcriptome data. This could indicate that the genes in the pathway are not up or down regulated in low or high phosphate conditions.

Table 1: Compiled list of all *Eutrema salsugineum* genes that were found to be involved in the glycolysis IV pathway that are involved in both the cytosolic and non-phosphorylating pathways.

Step in Glycolysis IV	Eutrema Gene
fructose 1,6-bisphosphate → D-glyceraldehyde 3-phosphate	Thhalv10000191m.g Thhalv10000915m.g Thhalv10010492m.g Thhalv10013921m.g Thhalv10016856m.g Thhalv10025379m.g Thhalv10025556m.g
3-phospho-D-glyceric acid → 2-phospho-D-glycerate	Thhalv10004074m.g Thhalv10007256m.g Thhalv10015179m.g Thhalv10020418m.g

Table 2: Compiled list of all *Eutrema salsugineum* genes that were found to be involved in the glycolysis IV pathway that are specific to the cytosolic pathway.

Step in Glycolysis IV	Eutrema Gene
D-glyceraldehyde 3-phosphate → 1,3-bisphospho-D-glycerate NAD^+ + phosphate → H^+ + NADH	Thhalv10004349m.g Thhalv10007716m.g Thhalv10007809m.g Thhalv10008131m.g Thhalv10018604m.g Thhalv10021083m.g Thhalv10021788m.g
1,3-bisphospho-D-glycerate → 3-phospho-D-glycerate ADP → ATP	Thhalv10018657m.g Thhalv10020621m.g

Table 3: Compiled list of all *Eutrema salsugineum* genes that were found to be involved in the glycolysis IV pathway that are specific to the non-phosphorylating pathway.

Step in Glycolysis IV	Eutrema Gene
D-glyceraldehyde 3-phosphate → glycerate-3-phosphate	Thhalv10000249m.g Thhalv10010654m.g
D-glyceraldehyde 3-phosphate → 3-phospho-D-glyceric acid H_2O + $NADP^+$ → H^+ + NADPH	Thhalv10000267m.g

Discussion

This thesis examined *Eutrema*'s usage of Pi, and more specifically how effectively *Eutrema* is able to use the non-phosphorylating glycolysis pathway to maintain its Pi levels. Both the Yukon and Shandong ecotype were tested and their rates of activity of cGAPDH and NP-GAPDH measured and compared.

The initial plan for this project was to grow fresh Yukon and Shandong plants on soil from seeds and use new plant material in the assays, but complications with a fungus in the soil stunted plant development too significantly for healthy growth to occur. The stored tissue from Jess Latimer that was used instead had been well kept and catalogued, which allowed the project to remain on the same analytical track. If there had been more time to grow more plants, it would have been interesting to compare the assay results of the fresh plant material to the frozen material both as a true biological replicate and to see if freezing the tissue diminished enzyme activity.

The results of the cGAPDH assay were mostly as expected, with the Yukon ecotype's rates of activity falling in the same range and order of magnitude as Velasco's results (2017) and displaying the same trend of +Pi shoots showing greater rates of activity than -Pi shoots. The Shandong ecotype, which had not been assayed for cGAPDH activity before, displayed similar results to the Yukon ecotype in terms of both rates of activity and comparison between -Pi and +Pi shoots. These results make logical sense, given that a plant that has access to more Pi will be more capable of using it in metabolic processes, but also suggests that both ecotypes are severely hindered in their ability to use the cGAPDH pathway in Pi-deficient environments.

When the NP-GAPDH assay was first attempted with spare desalted shoot material, no activity was seen for either the water controls or plant material trials. Extensive troubleshooting found that the aldolase that had been used had died, so a new sample had to be located. One liquid sample from 2015 was found and it was able to produce results, but they were lower than Velasco's results (2017). A second sample in crystal form from 2012 was sourced from another lab, and its results were much closer to those found in the literature. Since the aldolase was coming from a crystalline source instead of being stored in solution, it was possible that there were contaminants that were causing a false positive increase in activity. To test this, a blank trial of the NP-GAPDH assay was run. A flat-bottom 96-well MicroTest Plate was prepared using the proper assay soup and volumes of a standard NP-GAPDH assay, but the 10 µL of desalted plant material was replaced with water to determine if the aldolase was reacting with something else that could be absorbed at the same wavelength as the NADPH. The plate was then measured at 340 nm in the Multiskan Spectrum 1500. This trial showed no difference in absorbance between the water controls and the ones initiated with F16P2, indicating that at the very least the aldolase was not generating its own activity.

The NP-GAPDH data was interesting, because the gFW data and mgprot data showed conflicting results. The gFW data reported rates that matched with the expected outcome and previous literature, where -Pi plants displayed a greater capacity to use the bypass than +Pi plants, whereas the mgprot data reported that Yukon -Pi plants had almost no capacity to use the bypass, which directly contradicts the findings of Velasco (2017). These results do not make biological sense, because a plant with limited access to Pi that is known to be capable of using this bypass and surviving heartily in these conditions should be using the pathway to a greater extent than the plants that have access to Pi. An analysis of the amount of protein per gFW in

each sample found that protein data for Yukon shoots had inconsistent and strange values, possibly indicating a problem with the Bradford's assay. Therefore, the results and trends reported by the gFW data should be prioritized over the mgprot results and trends until further trials can be performed to verify both the protein data and the NP-GAPDH data.

Examining the gFW data showed interesting results for Shandong plant enzyme activity, as it showed a similar trend to the gFW data in that -Pi plants had a greater capacity to use the bypass than +Pi plants. However, the variation between the -Pi and +Pi treatments was less pronounced in Shandong plants than in Yukon plants, possibly indicating that Shandong plants prefer to use the bypass constantly rather than only when necessary.

The genetic makeup of the bypass pathway could contribute to its more subdued role in *Eutrema*'s metabolic processes. Only three genes are involved in the NP-GAPDH pathway, with two of them being responsible for turning glycerone phosphate into D-glyceraldehyde 3-phosphate and only one being responsible for turning D-glyceraldehyde 3-phosphate into 3-phospho-D-glycerate and $NADP^+$ into NADPH. If these three genes are under-expressed or inhibited for any reason, then the pathway will generate less activity and be less productive. Unfortunately, gene expression was not able to be determined or analyzed from the available transcriptome data due to none of the identified genes being listed in the accessible data, so further research in this area will be required. It is possible that these genes are not up or down regulated in varying levels of Pi or nitrogen, which the transcriptome data was looking into.

Furthermore, the larger number of genes involved in the cGAPDH pathway could contribute to some of the variation seen in the assay results. Much like how different plants and even leaves can have different rates of protein from each other, if more genes involved in one

step are active or have been active in one plant than in another, the amount of activity that will be seen in analysis will be different as well.

To further investigate the role of the NP-GAPDH pathway in *Eutrema*, more biological replicates and more technical replicates should first be performed to support the evidence shown here that it is perhaps not as essential as once thought. Analysis of the genes encoding the NP-GAPDH pathway and their prevalence within both *Eutrema* ecotypes and comparison between wild type plants and laboratory grown plants might also be an interesting direction of study to see if and how their expression changes.

Conclusion

This project aimed to learn more about the purpose of the NP-GAPDH pathway in *Eutrema* in both the Yukon and Shandong ecotypes in Pi sufficient and deficient environments. It was found that the Shandong ecotype displayed a greater capacity to use the bypass than the Yukon ecotype. As the Shandong ecotype tends to be more sensitive to abiotic conditions such as drought and nutrient deficiency, this discovery could possibly indicate that the bypass is not essential for *Eutrema*'s ability to survive in extreme environments. A further investigation of this bypass through either additional testing or more direct genetic analysis would help to support these findings and solidify the understanding of the purpose of the bypass. If the pathway is able to serve a significant role in helping plants overcome Pi deficiency, then it may be a good option to investigate for wider crop application. If its role is much smaller, then alternative pathways should be investigated.

References

Amtmann, A., 2009. Learning from Evolution: Thellungiella Generates New Knowledge on Essential and Critical Components of Abiotic Stress Tolerance in Plants. *Molecular Plant*, 2(1), pp.3–12. https://doi.org/10.1093/mp/ssn094.

Ariga, H., Tanaka, T., Ono, H., Sakata, Y., Hayashi, T. and Taji, T., 2015. CSP41b, a protein identified via FOX hunting using Eutrema salsugineum cDNAs, improves heat and salinity stress tolerance in transgenic Arabidopsis thaliana. *Biochemical and Biophysical Research Communications*, 464(1), pp.318–323. https://doi.org/10.1016/j.bbrc.2015.06.151.

Arutyunov, D.Y. and Muronetz, V.I., 2003. The activation of glycolysis performed by the non-phosphorylating glyceraldehyde-3-phosphate dehydrogenase in the model system. *Biochemical and Biophysical Research Communications*, 300(1), pp.149–154. https://doi.org/10.1016/S0006-291X(02)02802-4.

Bradford, M.M., 1976. A rapid and sensitive method for the quantitation of microgram quantities of protein utilizing the principle of protein-dye binding. *Analytical Biochemistry*, 72, pp.248–254. https://doi.org/10.1006/abio.1976.9999.

Givan, C.V., 1999. Evolving concepts in plant glycolysis: two centuries of progress. *Biological Reviews*, 74(3), pp.277–309. https://doi.org/10.1017/S0006323199005344.

Goodstein, D.M., Shu, S., Howson, R., Neupane, R., Hayes, R.D., Fazo, J., Mitros, T., Dirks, W., Hellsten, U., Putnam, N. and Rokhsar, D.S., n.d. *Gene Report: Thhalv10000267m.g: Phytozome*. Available at: <https://phytozome-next.jgi.doe.gov/report/gene/Esalsugineum_v1_0/Thhalv10000267m.g> [Accessed 27 February 2024].

Griffith, M., Timonin, M., Wong, A.C.E., Gray, G.R., Akhter, S.R., Saldanha, M., Rogers, M.A., Weretilnyk, E.A. and Moffatt, B., 2007. Thellungiella: an Arabidopsis-related model plant adapted to cold temperatures. *Plant, Cell & Environment*, 30(5), pp.529–538. https://doi.org/10.1111/j.1365-3040.2007.01653.x.

Guevara, D.R., Champigny, M.J., Tattersall, A., Dedrick, J., Wong, C.E., Li, Y., Labbe, A., Ping, C.-L., Wang, Y., Nuin, P., Golding, G.B., McCarry, B.E., Summers, P.S., Moffatt, B.A. and Weretilnyk, E.A., 2012. Transcriptomic and metabolomic analysis of Yukon Thellungiella plants grown in cabinets and their natural habitat show phenotypic plasticity. *BMC plant biology*, 12, p.175. https://doi.org/10.1186/1471-2229-12-175.

Hurley, B.A., Tran, H.T., Marty, N.J., Park, J., Snedden, W.A., Mullen, R.T. and Plaxton, W.C., 2010. The Dual-Targeted Purple Acid Phosphatase Isozyme AtPAP26 Is Essential for Efficient Acclimation of Arabidopsis to Nutritional Phosphate Deprivation. *Plant Physiology*, 153(3), pp.1112–1122. https://doi.org/10.1104/pp.110.153270.

Ito, F., Chishiki, H., Fushinobu, S. and Wakagi, T., 2012. Comparative analysis of two glyceraldehyde-3-phosphate dehydrogenases from a thermoacidophilic archaeon, Sulfolobus tokodaii. *FEBS Letters*, 586(19), pp.3097–3103. https://doi.org/10.1016/j.febslet.2012.07.059.

Kazachkova, Y., Eshel, G., Pantha, P., Cheeseman, J.M., Dassanayake, M. and Barak, S., 2018. Halophytism: What Have We Learnt From Arabidopsis thaliana Relative Model Systems? *Plant Physiology*, 178(3), pp.972–988. https://doi.org/10.1104/pp.18.00863.

Kazachkova, Y., Khan, A., Acuña, T., López-Díaz, I., Carrera, E., Khozin-Goldberg, I., Fait, A. and Barak, S., 2016. Salt Induces Features of a Dormancy-Like State in Seeds of Eutrema (Thellungiella) salsugineum, a Halophytic Relative of Arabidopsis. *Frontiers in Plant Science*, [online] 7. Available at: <https://www.frontiersin.org/articles/10.3389/fpls.2016.01071> [Accessed 1 October 2023].

Khanal, N., Bray, G.E., Grisnich, A., Moffatt, B.A. and Gray, G.R., 2017. Differential Mechanisms of Photosynthetic Acclimation to Light and Low Temperature in Arabidopsis and the Extremophile Eutrema salsugineum. *Plants*, 6(3), p.32. https://doi.org/10.3390/plants6030032.

Lv, S., Wang, D., Jiang, P., Jia, W. and Li, Y., 2021. Variation of PHT families adapts salt cress to phosphate limitation under salinity. *Plant, Cell & Environment*, 44(5), pp.1549–1564. https://doi.org/10.1111/pce.14027.

MacLeod, M.J.R., Dedrick, J., Ashton, C., Sung, W.W.L., Champigny, M.J. and Weretilnyk, E.A., 2015. Exposure of two Eutrema salsugineum (Thellungiella salsuginea) accessions to water deficits reveals different coping strategies in response to drought. *Physiologia Plantarum*, 155(3), pp.267–280. https://doi.org/10.1111/ppl.12316.

Matsubara, K., Yokooji, Y., Atomi, H. and Imanaka, T., 2011. Biochemical and genetic characterization of the three metabolic routes in Thermococcus kodakarensis linking glyceraldehyde 3-phosphate and 3-phosphoglycerate. *Molecular Microbiology*, 81(5), pp.1300–1312. https://doi.org/10.1111/j.1365-2958.2011.07762.x.

Plaxton, W.C., 1990. Glycolysis. *Methods in Plant Biochemistry*, 3, pp.145–173.

Plaxton, W.C. and Tran, H.T., 2011. Metabolic Adaptations of Phosphate-Starved Plants. *Plant Physiology*, 156(3), pp.1006–1015. https://doi.org/10.1104/pp.111.175281.

Rius, S.P., Casati, P., Iglesias, A.A. and Gomez-Casati, D.F., 2006. Characterization of an Arabidopsis thaliana mutant lacking a cytosolic non-phosphorylating glyceraldehyde-3-phosphate dehydrogenase. *Plant Molecular Biology*, 61(6), pp.945–957. https://doi.org/10.1007/s11103-006-0060-5.

Summers, P.S. and Weretilnyk, E.A., 1993. Choline Synthesis in Spinach in Relation to Salt Stress. *Plant Physiology*, 103(4), pp.1269–1276. https://doi.org/10.1104/pp.103.4.1269.

Vance, C.P., Uhde-Stone, C. and Allan, D.L., 2003. Phosphorus acquisition and use: critical adaptations by plants for securing a nonrenewable resource. *New Phytologist*, 157(3), pp.423–447. https://doi.org/10.1046/j.1469-8137.2003.00695.x.

Velasco, V.M.E., 2017. *Traits Underlying Phosphorus Use By The Extremophyte Eutrema Salsugineum*. McMaster University.

Velasco, V.M.E., Irani, S., Axakova, A., da Silva, R., Summers, P.S. and Weretilnyk, E.A., 2019. Evidence that tolerance of Eutrema salsugineum to low phosphate conditions is hard-wired

by constitutive metabolic and root-associated adaptations. *Planta*, [online] 251(1). https://doi.org/10.1007/s00425-019-03314-z.

Velasco, V.M.E., Mansbridge, J., Bremner, S., Carruthers, K., Summers, P.S., Sung, W.W.L., Champigny, M.J. and Weretilnyk, E.A., 2016. Acclimation of the crucifer Eutrema salsugineum to phosphate limitation is associated with constitutively high expression of phosphate-starvation genes. *Plant, Cell & Environment*, 39(8), pp.1818–1834. https://doi.org/10.1111/pce.12750.

Wang, D., Lv, S., Jiang, P. and Li, Y., 2017. Roles, Regulation, and Agricultural Application of Plant Phosphate Transporters. *Frontiers in Plant Science*, [online] 8. Available at: <https://www.frontiersin.org/articles/10.3389/fpls.2017.00817> [Accessed 1 October 2023].

Yang, S., Zhao, Y. and Wang, J., 2020. Function and application of the Eutrema salsugineum PHT1;1 gene in phosphate deficiency stress. *Plant Biology*, 22(6), pp.1133–1139. https://doi.org/10.1111/plb.13169.

Yeo, M.T.S., Carella, P., Fletcher, J., Champigny, M.J., Weretilnyk, E.A. and Cameron, R.K., 2015. Development of a Pseudomonas syringae–Eutrema salsugineum pathosystem to investigate disease resistance in a stress tolerant extremophile model plant. *Plant Pathology*, 64(2), pp.297–306. https://doi.org/10.1111/ppa.12271.

Yin, J., Gosney, M.J., Dilkes, B.P. and Mickelbart, M.V., 2018. Dark period transcriptomic and metabolic profiling of two diverse Eutrema salsugineum accessions. *Plant Direct*, 2(2), p.e00032. https://doi.org/10.1002/pld3.32.

Zhang, Y., Kouril, T., Snoep, J.L., Siebers, B., Barberis, M. and Westerhoff, H.V., 2017. The Peculiar Glycolytic Pathway in Hyperthermophylic Archaea: Understanding Its Whims by Experimentation In Silico. *International Journal of Molecular Sciences*, 18(4), p.876. https://doi.org/10.3390/ijms18040876.